



Dissolved cobalt speciation and reactivity in the eastern tropical North Atlantic

Oliver Baars^{a,b,*}, Peter L. Croot^{a,c}

^a Marine Biogeochemistry, GEOMAR, Germany

^b Princeton University, USA

^c Earth and Ocean Sciences, School of Natural Sciences, National University of Ireland, Galway, Ireland



ARTICLE INFO

Article history:

Received 15 June 2014

Received in revised form 4 October 2014

Accepted 6 October 2014

Available online 28 October 2014

Keywords:

Marine cobalt cycle

Cobalt reducibility

Seawater cobalt complexes

Cobalt distribution

Trace metal speciation

Kinetics

Thermodynamics

Reactivity

Marine cobalt redox chemistry

ABSTRACT

Recent studies highlight the role of cobalt (Co) as an important micro-nutrient with a complex scavenged type oceanic distribution. To better understand the biogeochemical cycle of Co we investigate the distribution, speciation and reactivity of dissolved Co in the eastern tropical North Atlantic in the upper 800 m of the water column. For this purpose, we complement classical Co ligand titrations that require a thermodynamic equilibrium with evaluations of ligand-exchange kinetics and reducibility of potential Co(III) species. The experiments include additions of the artificial Co binding ligands dimethylglyoxime or Nioxime and detection by cathodic stripping voltammetry. We find two pools of Co compounds: a labile fraction that exchanges Co within minutes and a strong/inert fraction that does not react within a 24-h period. No intermediate, slowly exchanging fraction is observed. Detection window experiments to determine complex stability constants show that the labile Co fraction is weak and likely consists of Co(II) complexes with no detectable free Co(II) ligands. The fraction of inert Co is always highest at the depth of the chlorophyll-a maximum. Addition of the reductant ascorbate increases the fraction of Co with rapid ligand-exchange kinetics and indicates the presence of dissolved reducible Co(III). The apparent Co(III) reducibility is highest at the chlorophyll-a maximum and decreases in deeper waters. Our results are in agreement with phytoplankton and associated bacteria being a source of Co(III) species, such as vitamin B₁₂. The presented results have important implications for our understanding of the biological availability and the marine cycle of Co.

© 2014 Elsevier B.V. All rights reserved.

1. Introduction

Cobalt is the essential metal center in vitamin B₁₂ (Guillard and Cassie, 1963) and plays a role in proteins where it can substitute Zn in a variety of phytoplankton species (e.g. Carbonic Anhydrases, Alkaline Phosphatases) (Lane and Morel, 2005; Saito and Goepfert, 2008). In the marine environment, dissolved Co concentrations are in the low pico-molar range and may reach levels that can limit certain phytoplankton species and (co-)limit primary productivity (Bertrand et al., 2007; Panzeca et al., 2008; Saito and Moffett, 2002). Consistent with this role of Co, oceanic depth profiles are often nutrient type in the upper water column. However, the low solubility of inorganic Co(III) prevents accumulation in the deep oceans and contributes to the intermediate depth concentration maxima of dissolved Co that are observed in some ocean regions (Noble et al., 2008; Saito and Moffett, 2002). In particular, Co(II) may be co-oxidized by Mn oxidizing bacteria and subsequently precipitate with Mn oxides (Moffett and Ho, 1996). Reductive dissolution of Co(III) at the continental shelf and advection with oxygen

minimum zone waters may additionally contribute to the formation of intermediate depth maxima of Co in the open ocean (Noble et al., 2012; Saito et al., 2010).

Organic cobalt complexes in seawater can strongly affect abiotic and biotic reactions. Therefore, to understand the cycle of Co and its interaction with micro-organisms, it is important to unravel the speciation and reactivity of Co in the dissolved phase. Previous Co speciation studies have been performed using electrochemistry, whereby an artificial Co ligand is added that competes with natural Co ligands in the sample and its complex can be directly determined by adsorptive cathodic stripping voltammetry (AdCSV) (Ellwood and Van den Berg, 2001; Saito and Moffett, 2001). In that way, it has been shown that a significant fraction of Co may be bound to organic ligands that do not exchange the metal after overnight equilibration with the competing ligand dimethylglyoxime (DMG) (Noble et al., 2012; Saito et al., 2010), whereby the cyanobacteria *Prochlorococcus* and *Synechococcus* are among the possible sources of ligands (Saito et al., 2002, 2005). Additions of Co to the sample can be done to titrate unbound natural ligands and calculate conditional complex stability constants and ligand concentrations (Ellwood and Van den Berg, 2001; Saito and Moffett, 2001). Free Co ligands have been detected in only a subset of the examined regions and water masses, that were mainly located in the

* Corresponding author at: Princeton University, Department of Geosciences, Guyot Hall, Princeton, NJ 08544, USA. Tel.: +1 609 356 8195.
E-mail address: obaars@princeton.edu (O. Baars).

Subtropical Zone south of Africa and in the Subantarctic Zone (Bown et al., 2012; Ellwood et al., 2005).

Yet, little is known about the ligand-exchange kinetics of organic cobalt complexes or the reactivity of Co in redox reactions and the redox state of Co still remains controversial (Ellwood et al., 2005). These aspects may be important for the biological availability of Co as well as abiotic reactions in seawater. Inorganic Co is present as Co(II), due to the highly positive redox potential for the Co(II)/Co(III) couple ($E^0_{\text{Co(II)/Co(III)}} = 1.84 \text{ V}$) and the low solubility of inorganic Co(III) ($K_{\text{sp Co(OH)}_3} = 10^{-44.5}$ (Martell and Smith, 1976); $K_{\text{sp CoOOH}} = 10^{-50}$ (Hem et al., 1985)). However, organic complexes with Co(III) are typically much stronger than those with Co(II), such that the redox potential is lowered and Co(III) is favored in oxygenated waters. In addition to the stronger binding of Co(III) to organic ligands, the ligand-exchange kinetics are typically much slower (Soni and Soni, 2013). Thus, investigations into Co ligand exchange kinetics and the redox state of Co are required to better understand its biological availability and marine cycle.

In this work, we complement the classical thermodynamic-equilibrium Co titration approach by evaluation of Co ligand-exchange kinetics in samples collected in the eastern tropical North Atlantic using a highly sensitive catalytic AdCSV method (Baars and Croot, 2011). In addition, we assess the presence and reducibility of dissolved Co(III) in seawater using ascorbate as a reductant.

2. Materials and methods

2.1. Sample collection and treatment

The samples for this study were collected during the RV Meteor cruise M80/2 (Mindelo-Dakar) from November to December 2009 in the eastern tropical North Atlantic. Water samples for Co speciation were retrieved at five stations (Fig. 1) from eight depths within the upper 800 m of the water column using trace metal clean GO-FLO samplers (General Oceanics) attached to a Kevlar hydrowire. Upon recovery, the samplers were transferred into a class-5 clean room container and mounted on bottle racks. Sub-sampling proceeded into pre-cleaned 0.5 L Teflon bottles by filtration through 0.2 μm cartridges (Sartobran P, Sartorius) attached to the GO-FLOs using a slight overpressure of high purity nitrogen gas (Air Liquide, Nitrogen 5.0). All samples

were stored in the dark at room temperature until analysis aboard the ship. Aliquots for soluble nitrogen (N), nitrite (NO_2^-), and reactive phosphorous (PO_4^{3-}) were filtered in the same way and analyzed on the ship with a nutrient auto-analyzer (Grasshoff et al., 1999). A CTD probe, equipped with a fluorescence sensor, was mounted to a Niskin rosette and deployed at all Co speciation stations to acquire ancillary oceanographic data. Chlorophyll-a (chl-a) concentrations were estimated by calibration of the fluorescence sensor with individual chl-a measurements from the Niskin bottles. For this purpose, 250 mL samples were filtered onto glass fiber filters (GF/F Whatman) and extracted in 90% acetone prior to fluorometric (Turner AU-10) measurement of the chl-a concentration.

2.2. Reagents

All reagents were prepared in a laminar flow bench inside a class-5 clean room container and stored in pre-cleaned Teflon bottles. Sub-boiling quartz-still purified HCl (Q-HCl) was used for preparation of buffers and to acidify seawater samples. Stock solutions of dimethylglyoxime (DMG, 0.1 M, Fluka) and 1,2-cyclohexanedionedioxime (Nioxime, 100 μM , trace metal grade) were prepared in HPLC grade methanol (Fluka). Concentrated NH_4OH (25%, TraceSelect, Fluka) was used for the ammonia buffer and adjusted with Q-HCl and 18 M Ω resistivity water (MQ) to yield a 5 M solution of $\text{pH} = 9.2 \pm 0.1$. For the bromate stock solution, 3 g KBrO_3 (SigmaUltra, Sigma-Aldrich) was dissolved in 50 mL MQ to give a 0.36 M solution. A 0.1 M trace metal grade H_2O_2 solution (TraceSELECT Ultra, Sigma-Aldrich) was used for UV digestions. Co standards were prepared by dilution of a 1000 ppm Co stock solution (Waters, in 5% HNO_3) and acidification to $\text{pH} < 2$ using Q-HCl. EDTA stock solutions (trace metal grade, Sigma-Aldrich) were prepared in MQ and neutralized with NH_4OH . Stock solutions of L-ascorbic acid (0.1 M, TraceSELECT, Fluka) were prepared before each experiment by dissolution in MQ that was deoxygenated by purging with high purity N_2 for 5 min. Stock solutions of the ammonia buffer, DMG and KBrO_3 were prepared new at least every week. All pH values were measured on the NBS scale.

2.3. Cobalt analyses

Samples for total dissolved Co and Co speciation were analyzed on the ship within three days after collection of the sample. In that way, storage artifacts, that were previously observed in the tropical eastern South Atlantic oxygen minimum zone by a loss of total Co in samples that were shipped to the shore, were avoided (Noble et al., 2012). The dataset is available for download at the PANGAEA™ database (<http://www.pangaea.de>, doi:10.1594/PANGAEA.836145).

2.3.1. Total dissolved cobalt

Total dissolved Co concentrations were measured after UV digestion of organic Co ligands. For this purpose, 10 mL sample aliquots were transferred into pre-cleaned and sample-rinsed Teflon capped quartz tubes and acidified to $\text{pH} < 2$ with Q-HCl. H_2O_2 was added to a concentration of 200 μM and samples were then UV digested for 3 h by placing them in a circular setup around a central UV source (Pen-Ray, UVP). Analysis proceeded after cooling to room temperature ($\sim 1 \text{ h}$) by catalytic AdCSV as described previously (Baars and Croot, 2011). Briefly, the UV digested samples were transferred into a cleaned Teflon cell cup and buffered by addition of a $\text{NH}_3/\text{NH}_4\text{Cl}$ buffer (0.11 M, $\text{pH} = 8.7 \pm 0.1$). DMG (0.22 mM) and KBrO_3 (0.032 M) was added and the sample was purged with ultra-high purity nitrogen for 200 s for the first measurement and 20 s after standard additions or for replicate measurements. A potential of -0.60 V was applied for 88 s during the deposition step. The potential was then switched to -1.025 V for 2 s to minimize the Ni(HDMG) $_2$ peak that could overlap with the Co signal. After a quiescence period of 10 s, the potential was ramped from -0.60 V to -1.25 V using a square wave pulse modulation (frequency = 50 Hz; scan rate = 0.1275 V/s; pulse amplitude = 0.075 V; step potential = 2.55 mV). The height of

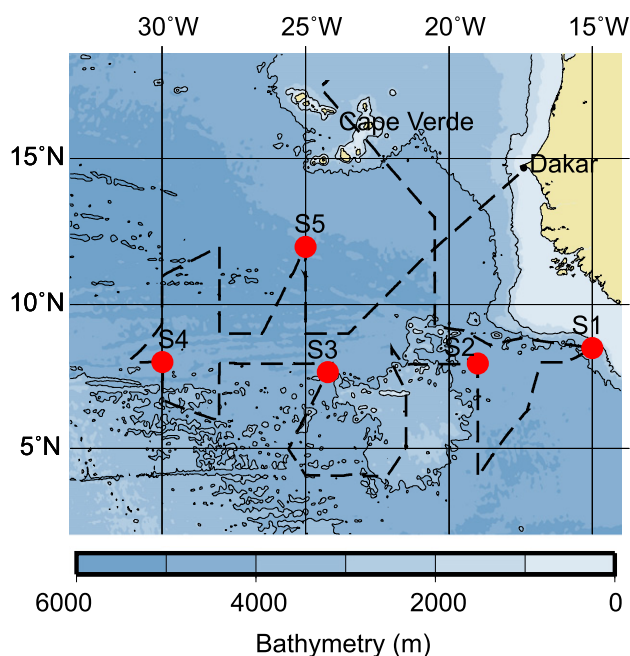


Fig. 1. Location of Co speciation stations during the RV Meteor expedition M80/2 (November–December 2009).

the Co peak was determined after baseline correction by subtraction of an exponential baseline from each voltammogram. The concentration of Co was calculated after 3–4 internal standard additions and each measurement was run in duplicate. After each analysis the Teflon cell was thoroughly cleaned by successively rinsing with ethanol, dilute Q-HCl and 0.1 mM DMG. After each rinsing step the cell was washed with MQ. At the beginning of each day a standard Co sample was measured to ensure the system was clean and to monitor Co blanks. Accuracy and precision of the method were evaluated with the GEOTRACES intercalibration samples SAFe S (intercalibration North Pacific 2004, surface seawater) and SAFe D2 (intercalibration North Pacific 2004, 1000 m). The results for SAFe S (7.1 ± 1.1 pM, $n = 10$) and SAFe D2 (44.9 ± 2.4 pM, $n = 10$) were in good agreement with the consensus values (SAFe S: 4.8 ± 1.2 pM; SAFe D2: 45.7 ± 2.9 pM; <http://www.geotraces.org/science/intercalibration/322-standards-and-reference-materials>) as previously reported (Baars and Croot, 2011).

2.3.2. Cobalt speciation and reactivity

A comprehensive Co speciation scheme was developed for this study that includes a set of three complementary experiments as shown in Fig. 2. In all experiments a competing Co ligand (DMG or Nioxime) is added to the samples and its complex is quantified by bromate catalyzed AdCSV.

1) Titration of natural Co ligands with added Co(II)

Methods for Co titrations of natural ligands with an added competing ligand and measurement by adsorptive cathodic stripping voltammetry (CLE-AdCSV) have been reported previously (Ellwood and Van den Berg, 2001; Saito and Moffett, 2001) and the theory has been discussed in detail (Zhang et al., 1990). Here, we use Nioxime as competing ligand, as described by Ellwood and Van den Berg (2001), with slight modifications to use bromate instead of nitrite as catalytic reagent to enhance the Co peak during detection. 10×10 mL seawater aliquots were poured into pre-cleaned and sample rinsed Teflon bottles and 80 mM ammonia buffer (final sample pH = 9.1 ± 0.1) was added. Eight Bottles were spiked with increasing Co(II) concentrations between 10–1000 pM and natural ligands in the samples were left to equilibrate with the added Co for 1 h. Subsequently, 2 μ M (S1) or 200 nM Nioxime (S2–5) was added to all bottles and the samples were left to equilibrate at room temperature for 1 d. After the equilibration period, the first sample was introduced into the cell (pre-cleaned by rinsing with

MQ, ethanol, MQ, dilute Q-HCl, MQ, 200 nM Nioxime, and MQ), 0.032 M bromate was added, and the measurement was started. The electrochemical method included a 200 s purge with N_2 before deposition at -0.7 V for 118 s followed by a potential switch to -0.96 V for 2 s to eliminate the interfering Ni signal. After a 10 s equilibration, the potential was ramped from -0.6 V to -1.2 V using a square wave modulation (frequency = 50 Hz, step potential = 2.55 mV, amplitude = 75 mV) and the Co peak height was determined after baseline correction by subtraction of an exponential baseline. Two replicates were measured for each bottle. The equilibrated bottles were measured in order of increasing added Co concentrations and no rinsing of the cell cup was done between measurements in a titration.

The stability of the cobalt complex with Nioxime was calibrated against EDTA by variation of the EDTA concentration in seawater with 1 nM added Co. The side reaction coefficient for Co complexed to Nioxime ($\alpha_{Co(Nioxime)_2}$) was calculated for each EDTA concentration according to Eq. (1) (Zhang et al., 1990):

$$\alpha_{Co(Nioxime)_2} = \frac{(\alpha_{Co'} + \alpha_{CoEDTA})X - \alpha_{Co'}}{1 - X} \quad (1)$$

with X being the ratio of the peak current at a given EDTA concentration to the peak current in the absence of EDTA. The inorganic side reaction coefficient $\alpha_{Co'}$ was previously reported to be 2.2 at pH = 9.1 (Ellwood and Van den Berg, 2001). α_{CoEDTA} is the side reaction coefficient for Co with EDTA with $\alpha_{CoEDTA} = \log K'_{CoEDTA} * [EDTA']$ and $\log K'_{CoEDTA} = 7.66$ (Ellwood and Van den Berg, 2001). The averaged results yield $\log \alpha_{Co(Nioxime)_2} = 5.2$ at 2 μ M Nioxime and $\log \alpha_{Co(Nioxime)_2} = 4.3$ at 200 nM Nioxime. Ellwood and Van den Berg (2001) report $\log \alpha_{Co(Nioxime)_2} = 4.75$ at 200 nM Nioxime. The difference can be explained by the experimental pH range of 9.0–9.2 as the complex stability of Co with Nioxime is strongly pH dependent with a two order of magnitude change in the conditional stability constant per pH unit (Bown et al., 2012; Saito and Moffett, 2001). The detection windows for the conditional stability constant of natural organic cobalt complexes (K'_{CoL}) associated with the two Nioxime concentrations are given in Table 1.

2) Ligand-exchange kinetics

The ligand-exchange reactivity for natural Co complexes was evaluated by addition of the competing ligand DMG (0.22 mM) at pH = 9.1 ± 0.1 (NH_3/NH_4Cl buffer, 0.08 M) whereby the sample was either measured immediately in the voltammetric cell ('labile Co', S1–S5) or after a reaction time of 24 h in pre-cleaned and sample-rinsed Teflon bottles ('exchangeable Co', S1). After the given reaction time, the measurement of the labile and exchangeable Co concentrations proceeded by addition of $KBrO_3$ (0.032 M) and internal standard additions analogous to the determination of total dissolved Co. Using a reported 2 order of magnitude change in the conditional stability constant of the Co–DMG complex ($K'_{Co(HDMG)_2}$) per pH unit (Saito and Moffett, 2001) and a published stability constant for the Co–DMG complex at pH = 8.7 ($\log K'_{Co(HDMG)_2} = 12.85$ (Zhang et al., 1990)), the $\log K'_{Co(HDMG)_2}$ in this study can be calculated to 13.65. With $\alpha_{Co(HDMG)_2} = K'_{Co(HDMG)_2} * [DMG]^2$, the side reaction coefficient for the Co–DMG complex is $\log \alpha_{Co(HDMG)_2} = 6.4$.

Table 1

Detection windows for conditional stability constants of natural organic cobalt complexes ($\log K'_{CoL}$) in this study assuming a ligand concentration of 50 pM.

Competing ligand	$\log \alpha$	Detection window for $\log K'_{CoL}$
[DMG] = 220 μ M	6.4 ^a	15.7–17.7
[Nioxime] = 2 μ M	5.2 ^b	14.5–16.5
[Nioxime] = 200 nM	4.3 ^b	13.6–15.6

^a Calculated.

^b Measured.

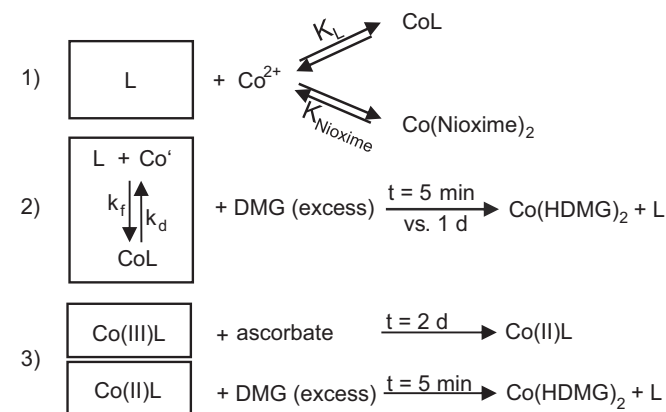


Fig. 2. Co speciation and reactivity experiments in this study: (1) Co(II) titrations to measure Co ligand (L) concentrations and complex stability constants (K) by equilibration with Nioxime as competing ligand; (2) Reactivity measurements of natural Co complexes (CoL) for ligand-exchange with the competing ligand DMG added at high concentrations to prevent the back reaction and to quantitatively complex reactive Co; (3) Reactivity measurements for the reduction of Co(III) species with added ascorbate. If organic Co(III) complexes exist in the sample that are inert for ligand-exchange reactions, reduction with ascorbate may increase the labile Co pool.

Table 1 summarizes the side reaction coefficient and associated conditional stability constant detection windows for natural organic Co complexes (K'_{CoL}) with an assumed ligand concentration of 50 pM.

- 3) Reducibility of potential organic Co(III) complexes 30 mL of sample was measured into pre-cleaned and sample rinsed Teflon bottles and deoxygenated by purging with high purity N_2 for 2 min. EPPS (1 mM, 30 μL of a 1 M stock) and L-ascorbate (200 μM , 60 μL of a 0.1 M stock) were added to give a sample pH of 7.7 ± 0.1 . The Teflon bottles were double bagged and left to react for 2 days at room temperature in the dark. At the end of the reaction time, a 10 mL sample aliquot was transferred into the cell cup and the reagents $\text{NH}_3/\text{NH}_4\text{Cl}$ buffer (0.08 M), DMG (0.22×10^{-3} M) and KBrO_3 (0.032 M) were added prior to measurement with the same method that was used for determination of total dissolved Co. The sample pH after addition of the $\text{NH}_3/\text{NH}_4\text{Cl}$ buffer was 9.0 ± 0.1 .

3. Results and discussion

3.1. Hydrography

The upper water column in the study area is strongly stratified (Fig. 3) and shows a single chlorophyll-a (chl-a) maximum at the depth of the nutricline (40–70 m), with peak chl-a concentrations between 0.65–1.01 $\mu\text{g L}^{-1}$. Linked to the shallow nutricline is a close correlation between N and P concentrations. Macronutrient distributions and dynamics have been closely investigated by Hauss et al. (2013) during this cruise. Lower near-surface N and P concentrations as well as depth integrated chl-a stocks are reported for the western stations, as seen at S4 in this study, while coastal upwelling provides macronutrients and drives higher primary productivity in the eastern part of the study area (Figs. 4 and 5). The center of the study area (S3) contains also high chl-a stocks, possibly due to elevated diapycnal fluxes there (Banyte et al., 2012; Hauss et al., 2013). Associated with the coastal upwelling system in the North Atlantic is an oxygen minimum zone (OMZ) (Capone and Hutchins, 2013) that we observe between 100–700 m. The O_2 concentrations in the OMZ core at ~400 m reach 40–55 $\mu\text{mol kg}^{-1}$, with lower levels closer to the African coast (Fig. 3). Overall however, changes in hydrography, nutrient concentrations and biological activity in the depth profiles between the stations in the study area are relatively small.

3.2. Distribution of total dissolved Co

Total dissolved Co concentrations are always lowest in the surface sample (12–30 pM) and show a characteristic local sub-surface maximum (60–86 pM) at all stations between 90–120 m that corresponds to the depth of a local O_2 minimum at the base of the oxycline (Figs. 4, 5A). The concentrations of Co in the upper 200 m of the water column increase from the station furthest offshore (S4) towards the continental shelf (S1) and this increase corresponds to overall lower O_2 concentrations near the continent and higher P concentrations that are supplied by upwelling. A second, deeper local Co maximum is found at 400 m in the OMZ core for S1, S3, and S4 (Figs. 4, 5A).

There is an inverse correlation between Co and O_2 throughout the water column (Fig. 7, $R^2 = 0.57\text{--}0.96$), suggesting that dissolved Co may be supplied with OMZ waters. An inverse Co vs. O_2 correlation was also previously observed in the OMZ of the eastern tropical South Atlantic with total Co concentrations of ~130 pM at 50 $\mu\text{mol kg}^{-1}$ O_2 , whereby coastal reductive dissolution of Co is likely to supply Co to these waters (Noble et al., 2012). An analogous source may be hypothesized for the local Co concentration maxima at the O_2 minimum depths in this study. However, the concentration of Co in the OMZ core in this study is significantly lower (~80 pM at 50 $\mu\text{mol kg}^{-1}$ O_2). A known difference between the two oceanic regions are higher O_2 minimum concentrations in the North Atlantic OMZ compared to the South Atlantic OMZ (Karstensen et al., 2008). Thus, the ‘tipping point’ redox potential for Co mobilization by reductive dissolution of particulate Co(III) in shelf-sediments (Johnson et al., 1988) may be less frequently reached in the North Atlantic and explain the less pronounced Co concentration maxima in the OMZ core.

There is also a significant correlation between Co and P in the upper 400 m (Fig. 7, $R^2 = 0.58\text{--}0.92$), indicating that remineralization of organic matter can also contribute to the increase of Co below the nutricline, in agreement with the trace nutrient role of Co. It should be noted, that the deepest samples from 800 m show a decrease in the total Co concentration while P continues to increase, such that these samples do not fall on the Co vs. P correlation lines (Fig. 7). This decrease in dissolved Co below the OMZ can be explained by eventual scavenging of Co to particles. An important scavenging mechanism is thought to be the co-oxidation of Co(II) with Mn(II) by Mn oxidizing bacteria and precipitation of Co(III) with Mn oxides (Moffett and Ho, 1996; Saito and Moffett, 2001).

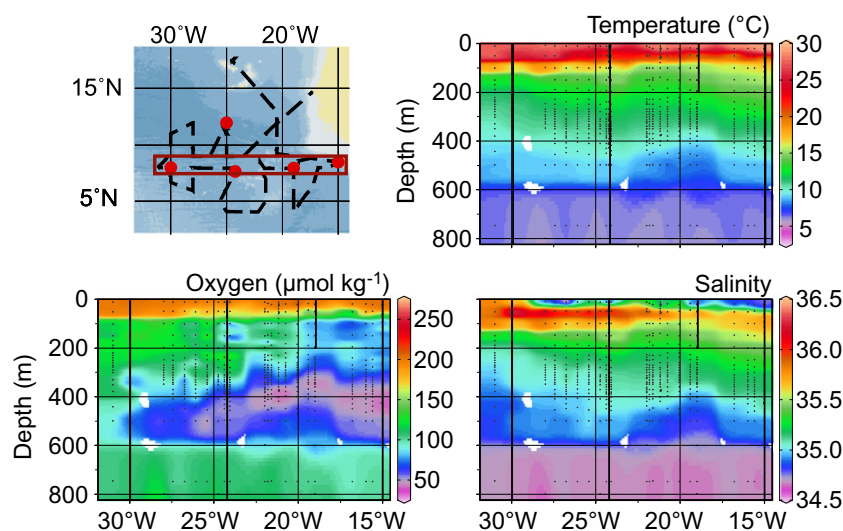


Fig. 3. Sections of temperature, salinity and oxygen in a west-east transect as shown in the map. The location of the Co speciation stations S1–S4 is indicated as red dots in the map and as vertical lines in the sections. All sections were created with Ocean Data View (Schlitzer, 2014).

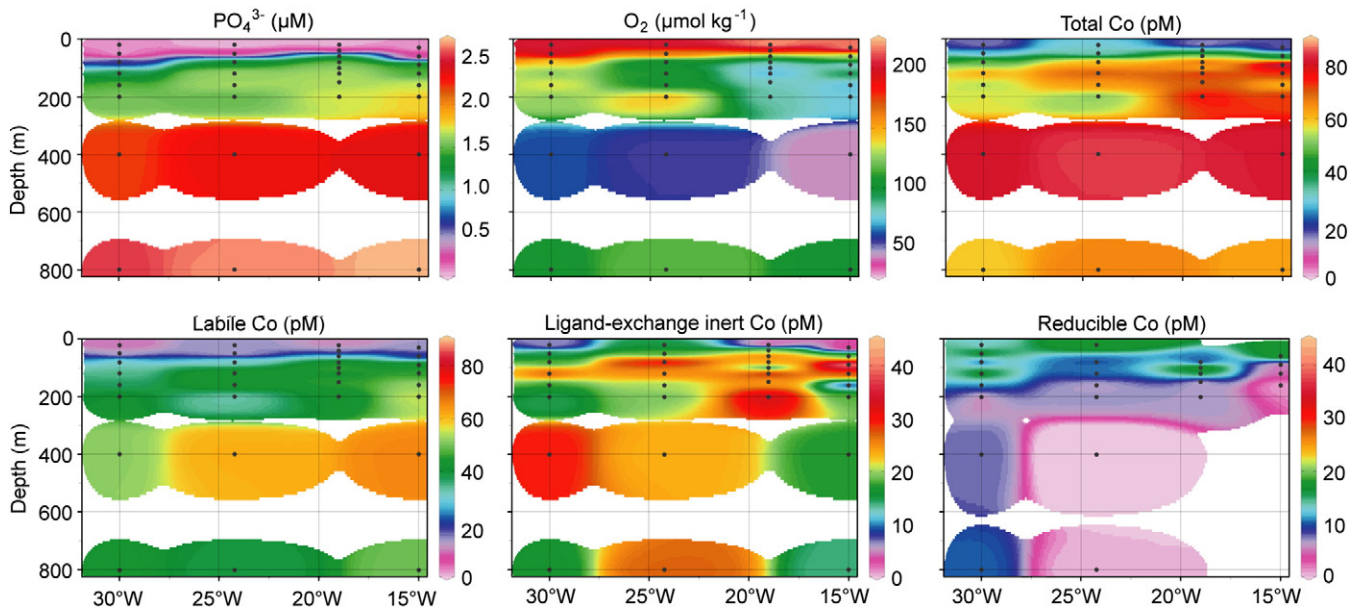


Fig. 4. Sections of PO₄³⁻, O₂, total dissolved Co, labile Co, ligand-exchange inert Co, and reducible Co (difference between Co measured after ascorbic acid reduction and labile Co) in a west-east transect with data from samples collected at S1–S4 (see map in Fig. 3).

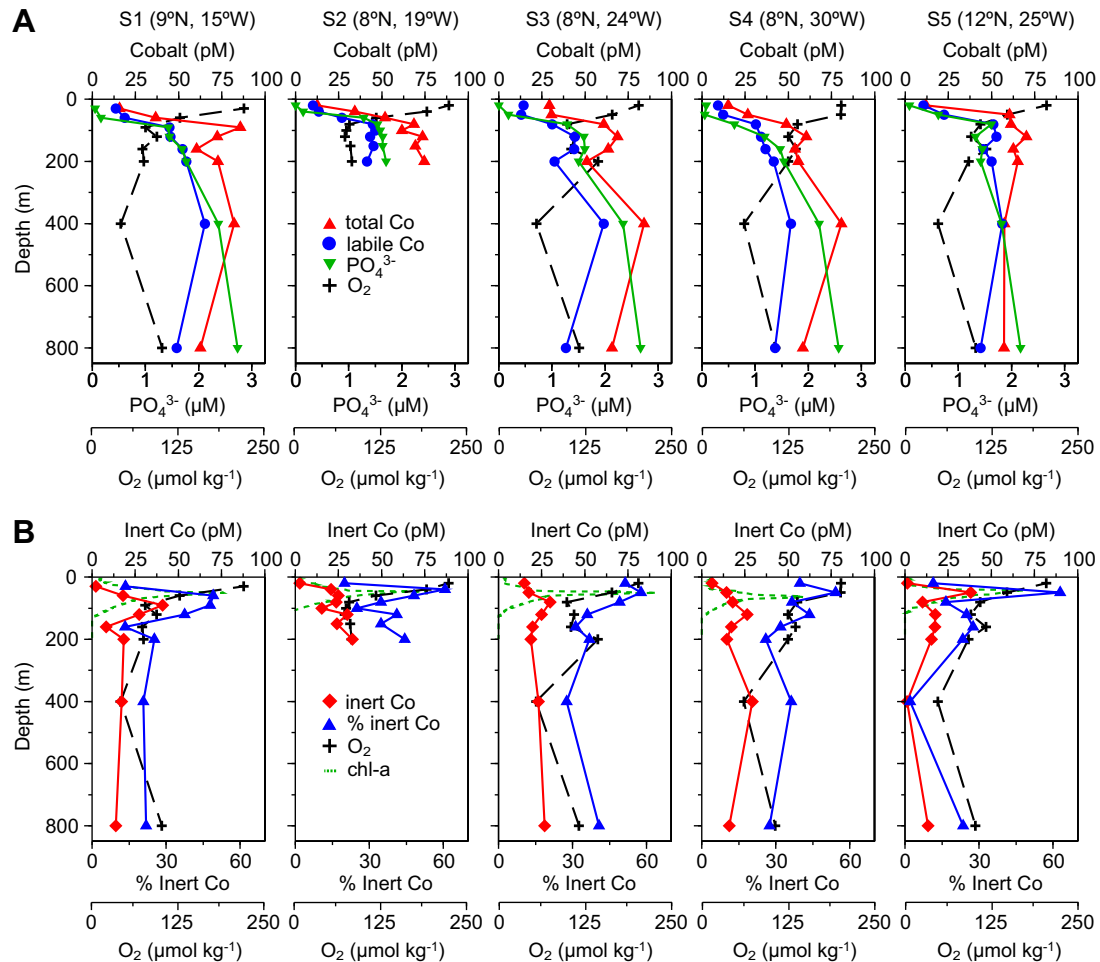


Fig. 5. (A) Depth profiles of total dissolved Co (▲), labile Co (●), phosphate (▼) and O₂ (+); (B) Depth profiles of ligand-exchange inert Co (◆), the %inert Co fraction of total Co (▲), chlorophyll-a (● ● ●, scale 0–1.1 µg L⁻¹) and O₂ (+).

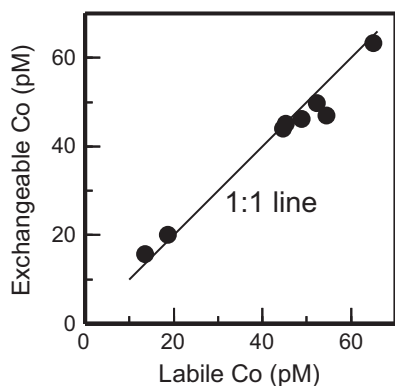


Fig. 6. Comparison of labile Co (measured immediately after addition of DMG) and exchangeable Co (measured after 24-h equilibration with DMG) with all samples collected at S1.

3.3. Ligand-exchange kinetics – labile and inert Co fractions

We evaluate the ligand-exchange reactivity for natural organic Co complexes with the added artificial ligand DMG at S1 by measurement of the Co–DMG complex concentration immediately after addition of DMG ('labile Co') and after a 24-h reaction time with DMG ('exchangeable Co'). We use a high concentration of DMG (220 μM) to increase the side reaction coefficient $\alpha_{\text{Co}(\text{HDMG})_2}$ and quantitatively complex reactive Co (Table 1). Exchangeable Co vs. labile Co concentrations from all samples in the depth profile at S1 fall on a 1:1 line (Fig. 6). At the same time, total Co concentrations are significantly higher than exchangeable or labile Co (Fig. 5A). Consequently, two separate pools of Co species are

found: a labile fraction that exchanges Co within the time of the measurement (<5 min) and an inert fraction that does not exchange Co within the 24-h equilibration period. No intermediate, slowly exchanging Co fraction is observed throughout the water column. Our results agree with previous findings of significant Co fractions that do not exchange with DMG or Nioxime after overnight equilibration (Bown et al., 2012; Ellwood et al., 2005; Noble et al., 2012; Saito et al., 2005). Yet, to our knowledge, this is the first evaluation of exchangeable Co concentrations as a function of reaction time and thus the first clear indication for labile and inert Co species without a significant contribution of slowly exchanging species within a 24-h equilibration period.

The inert pool consists of very strong complexes and/or complexes with slow ligand-exchange kinetics. At the experimental conditions, DMG is outcompeted at conditional stability constants of the natural complexes of $\log K'_{\text{CoL}} > 17.7$, assuming a ligand concentration of 50 μM (Table 1), which may be easily exceeded by Co(III) complexes but requires particularly strong Co(II) complexes (e.g. $\log K_{\text{Co(II)EDTA}} = 16.45$ vs. $\log K_{\text{Co(III)EDTA}} = 41.4$ (Martell and Smith, 1976)). In addition, strong octahedral Co(III) complexes are kinetically inert while Co(II) complexes are usually very labile (Soni and Soni, 2013), although slow Co(II) dissociation kinetics have been reported in some freshwater samples (Collins and Kinsela, 2010; Sekaly et al., 2002). Consequently, it is likely that the labile Co pool contains Co(II) species while the inert Co pool may include Co(III) or particularly inert Co(II) species.

These results have implications for the potential biological availability of Co, which requires a ligand-exchange reaction with Co uptake sites on the cell surface (Campbell et al., 2002). For example, a number of phytoplankton species, including diatoms, coccolithophores, or *Phaeocystis* are known to be able to substitute Zn(II) in various enzymes for Co(II) under low available Zn concentrations (Saito and Goepfert,

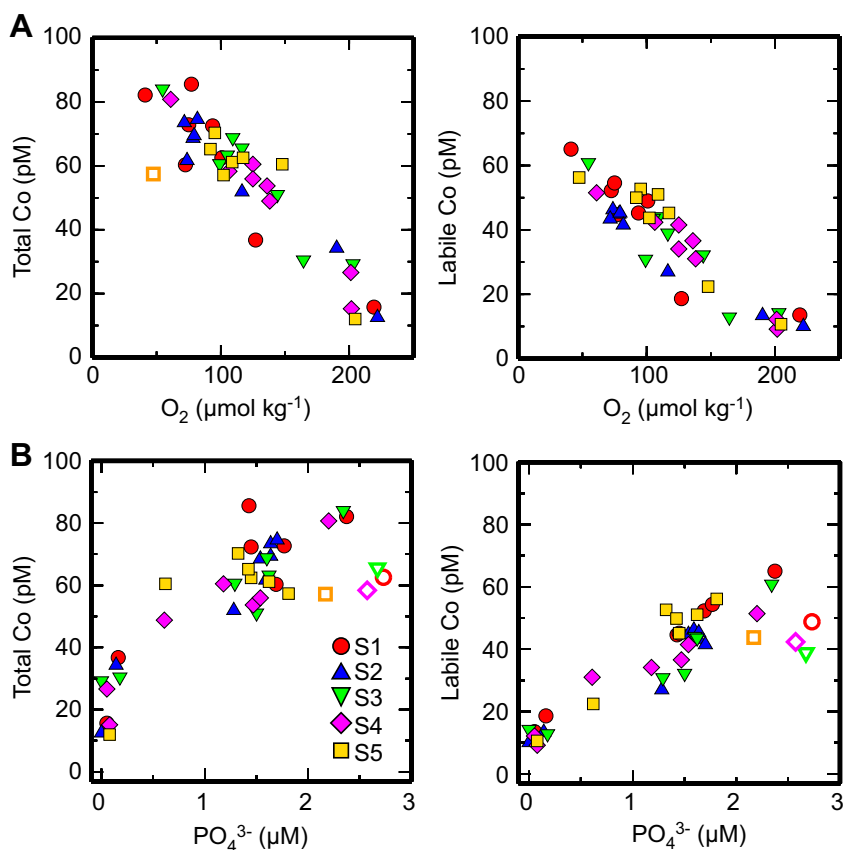


Fig. 7. (A) Plots of total Co vs. O_2 (linear regression $\text{Co}_{\text{total}} = -0.39 * \text{O}_2 + 10.3$, $R^2 = 0.88$) and labile Co vs. O_2 ($\text{Co}_{\text{labile}} = -0.30 * \text{O}_2 + 7.2$, $R^2 = 0.85$); (B) Plots of total Co vs. PO_4^{3-} and labile Co vs. PO_4^{3-} . Samples from 800 m are shown as open symbols in (B) and do not fall on the otherwise good correlation lines. The overall relations with all samples in the upper 400 m are: $\text{Co}_{\text{total}}(\text{pM}) = 26.1 * \text{P}(\mu\text{M}) + 24.5$ ($R^2 = 0.82$) and $\text{Co}_{\text{labile}}(\text{pM}) = 21.4 * \text{P}(\mu\text{M}) + 11.2$ ($R^2 = 0.90$).

Table 2
Detected Co concentrations with the competing ligands DMG and Nioxime. The detection window for the conditional complex stability of natural Co complexes associated with the different side reaction coefficients for the formation of the Co complex with the added competing ligand is given in Table 1.

Sample	Total Co (pM)	Labile Co		Exchangeable Co	
		[DMG] = 220 μ M		[DMG] = 220 μ M	
		$\log \alpha_{\text{Co(HDMG)}_2} = 6.4$		$\log \alpha_{\text{Co(HDMG)}_2} = 6.4$	
		Exchangeable		Exchangeable	
		Nioxime 2 μ M		Nioxime 0.2 μ M	
		$\log \alpha_{\text{Co(Nioxime)}_2} = 5.2$		$\alpha_{\text{Co(Nioxime)}_2} = 4.3$	
S1, 30 m	15.7	13.6	15.7	13.1	
S1, 60 m	36.7	18.7	20.1	19.5	
S2, 20 m	12.6	10.1			14
S2, 40 m	34.3	13.5			16.6
S2, 60 m	51.9	27			30
S2, 80 m	68.6	44.8			47.9

2008). In the context of our results, it is likely that the labile Co fraction is readily accessible for this purpose, while the ligand-exchange inert fraction may be unavailable.

3.4. Distribution of labile and ligand-exchange inert Co

As mentioned above, total Co distributions correlate with those of PO_4^{3-} and show an inverse correlation with O_2 . Similar relations are observed between labile Co and PO_4^{3-} or O_2 (Fig. 7). Yet, it is interesting to note that total Co follows O_2 more closely ($R^2 = 0.88$, all samples) than labile Co ($R^2 = 0.85$, all samples) while labile Co shows a stronger correlation with PO_4^{3-} ($R^2 = 0.90$, samples from the upper 400 m) than total Co ($R^2 = 0.81$, samples from the upper 400 m). The difference between total and labile Co is the concentration of ligand-exchange inert Co.

The distribution of inert Co reveals that the highest fraction of inert Co (49–63%) always occurs at the depth of the chl-a maximum between 40–70 m (Fig. 5B) and suggests that phytoplankton and associated bacteria can be a source of ligand-exchange inert Co species. These near-surface samples are largely responsible for the stronger correlation between labile Co and PO_4^{3-} compared to total Co and PO_4^{3-} . If inert Co is released by phytoplankton and associated bacteria but not available for uptake to the same extent as labile Co, it can accumulate at the chl-a maximum and explain the high fraction of inert Co. In this context, it has been previously reported that *Synechococcus* and *Prochlorococcus* can produce ligand-exchange inert Co species (Saito et al., 2002, 2005). For a discussion of possible species that could be associated with the inert Co fraction see section 'Possible source and identity of the ligand-exchange inert Co species'. In comparison to the samples from the chl-a maximum (40–70 m), the inert Co fraction in samples near the surface (20 m) is significantly lower (11–51%). UV or visible light irradiation is known to be able to induce ligand-to-metal-charge-transfer reactions in Co(III) complexes that can lead to the reduction of the metal center and oxidation of the ligand (Jothivenkatachalam et al., 2013).

Therefore, photolysis in surface waters may account for a decrease in inert Co(III) and an increase in labile Co(II) species that can explain the observed decrease in the inert Co fraction. The lower fraction of inert Co below the chl-a maximum may be explained by a preferential release of labile Co during remineralization as suggested by the correlated increase of labile Co and PO_4^{3-} (Fig. 7).

Below the chl-a maximum we find an absolute maximum in the inert Co concentration profiles which corresponds to a local oxygen minimum at the base of the main oxycline between 80–120 m at all stations (Figs. 4 and 5B). The source of inert Co in these waters can therefore be a release of inert Co species during early remineralization processes or the presence of bacteria that could catalyze the oxidation of Co(II) to Co(III) species or release inert organic cobalt complexes (see section 'Possible source and identity of the ligand-exchange inert Co species').

3.5. Titration of free Co ligands with added Co(II)

While the above experiments are in agreement with a reactive labile Co(II) pool in all samples, it remains unknown, if these Co(II) species consist of inorganic or organic complexes and if free ligands exist in solution. To answer these questions, we titrate seawater samples with Co(II) using Nioxime as competing ligand according to published protocols (Ellwood and Van den Berg, 2001). To test different detection windows, we use two Nioxime concentrations in this study (Table 2).

We obtain linear titration plots of detected Co vs. added Co (Fig. 8) in all samples and at both Nioxime concentrations indicating that no free Co ligands exist in solution with stability constants higher than the lowest end of the detection window ($\log K'_{\text{CoL}} > 13.6$, Table 1) assuming pM ligand concentrations. The intercept from the linear regression of the detected Co vs. added Co plot is the exchangeable Co concentration that is originally present in the samples (i.e. in samples that were not spiked with a Co standard). The exchangeable Co concentrations from the titrations are in good agreement with the measurements of labile or exchangeable Co with DMG as competing ligand (Table 2). This agreement between exchangeable Co concentrations with different competing ligands and different side reaction coefficients indicates that the exchangeable/labile Co pool contains inorganic Co(II) or weak organic Co(II) complexes that fall below the lowest detection window in this study. One explanation for this observation can be that Co(II) is outcompeted in the complex formation by other divalent trace metals that may be present at higher concentrations and may have higher organic complex stabilities according to the Irving–Williams-Series: $\text{Co(II)} < \text{Ni(II)} < \text{Cu(II)} > \text{Zn(II)}$. Our observations are in agreement with previous studies in the Sargasso Sea and the eastern equatorial North Pacific (Saito and Moffett, 2001; Saito et al., 2005) in which no free Co ligands were observed throughout the water column using DMG as competing ligand although excess ligands were reported in low dissolved Co waters in the Subtropical Zone south of Africa and in the Subantarctic Zone with Nioxime as competing ligand (Bown et al., 2012; Ellwood et al., 2005).

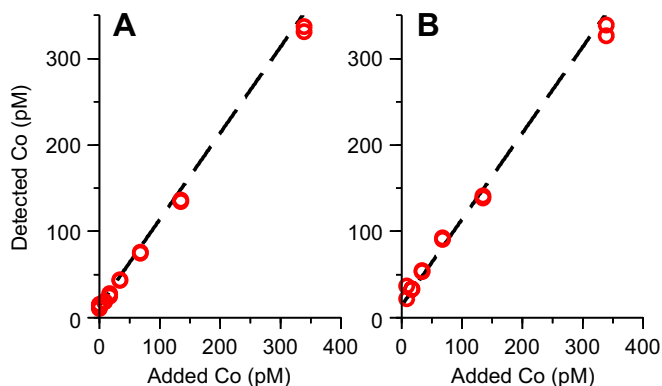


Fig. 8. Titration plot for A) a 30 m sample at S1 equilibrated with 2 μ M Nioxime and B) a 40 m sample at S2 with 0.2 μ M Nioxime.

3.6. Reducibility of potential Co(III) species

If the ligand-exchange inert Co pool consists of organic Co(III) complexes, it may be possible to reduce the metal center and thereby increase the Co pool that exchanges rapidly with DMG. The results show indeed significant reducible Co concentrations, calculated as difference between the concentration of Co measured after ascorbate reduction, and the labile Co concentration. The highest reducible concentration (16–22 pM) is always found in the sample with the highest chl-a concentration (S1, S3–5) and coincides with the highest fraction of ligand-exchange inert Co. In deeper waters (>200 m), reducible Co is lower, possibly as a result of the presence of more inert, aged species (Fig. 9).

While it cannot be excluded, that ascorbate may play a role in reactions during the electrochemical detection, the voltammetric baselines were little affected by the presence of ascorbate under the experimental conditions. The repeated observation of the described features at the different stations gives further confidence. To our knowledge, this is the first direct experimental evidence for dissolved Co(III) species in seawater. Previously, Saito and Moffett (2001) suggested the presence of organic Co(III) complexes in the Sargasso Sea because Co could not be exchanged with added excess Ni(II), as would be expected based on typically higher stability constants for organic Ni(II) complexes compared to organic Co(II) complexes. In addition, Co could not be removed from the complex, even at high DMG concentrations. Yet, Ellwood et al. (2005) made opposite observations in the Southern Ocean and found that Co could be removed from natural Co complexes at higher Nioxime concentrations.

Ascorbate is an important cellular reductant ($E^0 = 0.09$ V vs. SHE at pH = 7) (Foyer and Noctor, 2011) and its reducing properties have been studied with a number of transition metal complexes whereby the reactions proceed usually via an outer-sphere electron transfer (Lin et al., 2005). The redox potential of ascorbate is low enough to reduce typical organic Co(III) complexes, including, for example, Co(III)EDTA ($E^0 = 0.37$ V vs. SHE, 1 M NaClO₄), and a variety of related complexes (Lin et al., 2005; Ogino and Ogino, 1983). Ascorbate is also able to reduce vitamin B₁₂ (Nazhat et al., 1989). Ascorbate was previously used to measure incorporation of Co into Mn oxides by Mn oxidizing bacteria in seawater, whereby Mn oxides (Moffett and Ho, 1996) as well as

inorganic particulate Co(III) phases (Lee and Tebo, 1994) can be reduced. In this context, the reducible Co pool in this study may not only include organic Co(III) complexes but possibly also colloidal (<0.2 μm), inorganic phases. The reduction kinetics with ascorbate vary strongly between Co(III) complexes and are faster at higher pH values (the pH used in this study is 7.7). For example, using a reported rate constant for the reduction of Co(III)EDTA at pH = 9.5 (Lin et al., 2005), we calculate a pseudo first order reaction half-life time at the experimental ascorbate concentration of 3.7 h, while that for the reported reaction with a Co(III) Bis(terpyridyl) complex is 7.5 min at pH = 8.1 (Lin et al., 2005). In this context it is possible that some Co(III) complexes remain essentially inert for reduction with ascorbate within the experimental 2 day reaction time. These species may exist in the deeper samples in this study (>200 m) for which we observe low reducible concentrations but significant concentrations of ligand-exchange inert Co.

3.7. Possible source and identity of the ligand-exchange inert Co species

Our results show the highest inert Co fractions and high reducible Co(III) concentrations in samples close to the chl-a maximum. This suggests that phytoplankton and associated bacteria can be a source of ligand-exchange inert Co(III) species that are reducible with ascorbate. *Synechococcus* are known to release siderophores which may also be strong ligands for Co(III) as demonstrated with the siderophore desferrioxamine B (DFOB, log $K_{CoHDFOB} = 37.5$) (Duckworth et al., 2009). The N₂-fixing marine cyanobacterium *Crocospaera watsonii* is also found in our study region (Hewson et al., 2009) and may have the potential to produce siderophores (Hopkinson and Morel, 2009) though none have been detected yet. In the case of ligand production, it could be expected that excess unbound organic Co ligands may be found. Yet, no ligand excess is observed in our Co titration experiments.

Another possibility is that inert organic cobalt complexes are released by cells, either actively, passively or after cell breakage. An example for such species is the Co containing vitamin B₁₂ (Guillard and Cassie, 1963) which had been reported to be inert to metal-exchange (Boos et al., 1951). Various bacteria, including the cyanobacteria *Synechococcus* and *C. watsonii* are known to produce significant

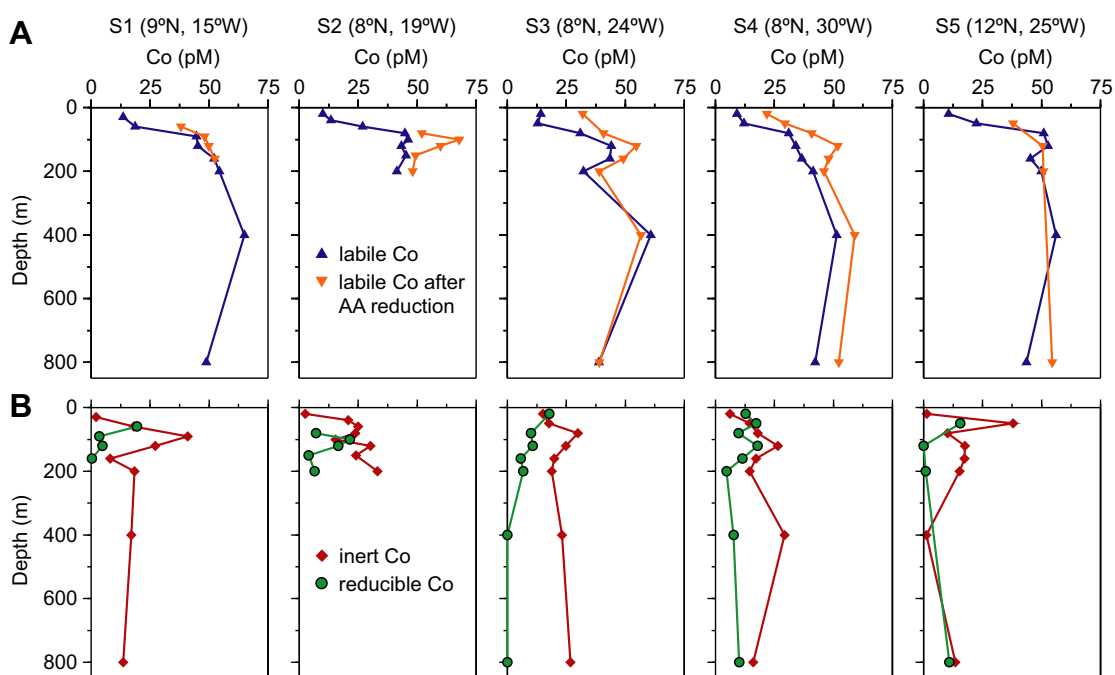


Fig. 9. Depth profiles of (A) Co concentrations measured after AA reduction (▼) together with labile Co (▲) and (B) reducible Co (difference between Co measured after AA reduction and labile Co) (●) with the concentration of ligand-exchange inert Co (◆).

amounts of B₁₂ (Bertrand et al., 2011; Bonnet et al., 2010; Carlucci and Bowes, 1970) and recent metagenomic analysis has suggested that archaea may also be responsible for B₁₂ production in some ocean regions (Doxey et al., in press). A few targeted measurements of B₁₂ and related species have been reported and show concentrations that reach the low pM range (e.g. Bonnet et al., 2013; Panzeca et al., 2009; Suárez-Suárez et al., 2011), whereby the measurements are complicated due to the potential presence of a variety of B₁₂ species and derivatives (Suárez-Suárez et al., 2011). However, based on the available data, it is possible that B₁₂ species may account for a significant fraction of the inert Co pool. The presence of vitamin B₁₂ would also be in agreement with the high reducible Co concentration at the chl-a maximum, as Co is known to be easily removed from B₁₂ via reduction with ascorbate (Nazhat et al., 1989). In surface waters above the chl-a maximum, we observe a low fraction of ligand-exchange inert Co that would be in agreement with photo-labile Co(III) species such as B₁₂ (Juzeniene and Nizauskaite, 2013). Yet, other organic Co(III) complexes may also be ligand-exchange inert, ascorbate-reducible and photo-labile as discussed above. In addition, colloidal inorganic Co(III) phases could be ligand-exchange inert and ascorbate-reducible and their formation could be mediated by the action of Mn oxidizing bacteria (see 'Reducibility of potential Co(III) species').

4. Summary and conclusions

The different experiments in this study included an evaluation of ligand-exchange kinetics, Co(II) titrations and a reducibility assay for Co(III) species. We find that the total dissolved Co pool comprises a rapidly-reacting, weakly-complexed Co(II) fraction and an inert/strong fraction that includes Co(III). We do not detect slowly exchanging Co throughout the water column. We did also not observe free ligands in the Co(II) titration experiments which may be a consequence of Co(II) being outcompeted by other divalent trace metals. Our observations of ligand-exchange inert, ascorbate-reducible and potentially photo-labile species at the chl-a maximum are in agreement with phytoplankton and associated bacteria being a source of organic Co(III) complexes, such as vitamin B₁₂ and related species. While the highest fraction of ligand-exchange inert Co is located at the chl-a maximum (40–70 m), we find an absolute concentration maximum of ligand-exchange inert Co at the base of the main oxycline (80–120 m) that corresponds to the depth of a local oxygen minimum. Further studies are required to elucidate, if the ligand-exchange inert Co(III) species may include also inorganic colloidal Co(III) oxides. Overall, our results provide new insights into dissolved Co speciation and reactivity in the oceans and have important implications for our understanding of the biological availability and the marine cycle of Co.

Acknowledgments

We thank the officers and crew of the RV Meteor. Work onboard the ship was supported by Anna Dammshäuser. Many thanks to Kerstin Nachtigall and Peter Streu (GEOMAR) for complementary macronutrient and trace metal analysis. Financial support was provided by the DFG Antarctic Program SPP 1158 via grant to PC (CR145/10-1) and by the Sonderforschungsbereich 754 "Climate-Biogeochemistry Interactions in the Tropical Ocean" (www.sfb754.de).

References

- Baars, O., Croot, P.L., 2011. Comparison of alternate reactants for pM level cobalt analysis in seawater by the use of catalytic voltammetry. *Electroanalysis* 23 (7), 1663–1670.
- Banyte, D., et al., 2012. Diapycnal diffusivity at the upper boundary of the tropical North Atlantic oxygen minimum zone. *J. Geophys. Res. Oceans* 117 (C9) (C09O16).
- Bertrand, E.M., et al., 2007. Vitamin B₁₂ and iron colimitation of phytoplankton growth in the Ross Sea. *Limnol. Oceanogr.* 52 (3), 1079–1093.
- Bertrand, E.M., Saito, M.A., Jeon, Y.J., Neilan, B.A., 2011. Vitamin B₁₂ biosynthesis gene diversity in the Ross Sea: the identification of a new group of putative polar B₁₂ biosynthesizers. *Environ. Microbiol.* 13 (5), 1285–1298.
- Bonnet, S., et al., 2010. Vitamin B-12 excretion by cultures of the marine cyanobacteria *Crocospaera* and *Synechococcus*. *Limnol. Oceanogr.* 55 (5), 1959–1964.
- Bonnet, S., et al., 2013. Geographical gradients of dissolved vitamin B₁₂ in the Mediterranean Sea. *Front. Microbiol.* 4.
- Boos, R.N., Rosenblum, C., Woodbury, D.T., 1951. The exchange stability of cobalt in vitamin B₁₂. *J. Am. Chem. Soc.* 73 (11), 5446–5447.
- Bown, J., Boye, M., Nelson, D.M., 2012. New insights on the role of organic speciation in the biogeochemical cycle of dissolved cobalt in the southeastern Atlantic and the Southern Ocean. *Biogeochemistry* 9 (7), 2719–2736.
- Campbell, P.G.C., Errécalde, O., Fortin, C., Hiriart-Baer, V.P., Vigneault, B., 2002. Metal bioavailability to phytoplankton—applicability of the biotic ligand model. *Comp. Biochem. Physiol. Pharmacol. C Toxicol. Endocrinol.* 133 (1–2), 189–206.
- Capone, D.G., Hutchins, D.A., 2013. Microbial biogeochemistry of coastal upwelling regimes in a changing ocean. *Nat. Geosci.* 6 (9), 711–717.
- Carlucci, A.F., Bowes, P.M., 1970. Production of vitamin B₁₂, thiamine, and biotin by phytoplankton. *J. Phycol.* 6 (4), 351–357.
- Collins, R.N., Kinsela, A.S., 2010. The aqueous phase speciation and chemistry of cobalt in terrestrial environments. *Chemosphere* 79 (8), 763–771.
- Doxey, A.C., Kurtz, D.A., Lynch, M.D.J., Sauder, L.A., Neufeld, J.D., 2014. Aquatic metagenomes implicate *Thaumarchaeota* in global cobalamin production. *ISME J.* <http://dx.doi.org/10.1038/ismej.2014.142> (in press).
- Duckworth, O.W., et al., 2009. The exceptionally stable cobalt(III)–desferrioxamine B complex. *Mar. Chem.* 113 (1–2), 114–122.
- Ellwood, M.J., Van den Berg, C.M.G., 2001. Determination of organic complexation of cobalt in seawater by cathodic stripping voltammetry. *Mar. Chem.* 75, 33–47.
- Ellwood, M.J., et al., 2005. Organic complexation of cobalt across the Antarctic Polar Front in the Southern Ocean. *Mar. Freshw. Res.* 56 (8), 1069–1075.
- Foyer, C.H., Noctor, G., 2011. Ascorbate and glutathione: the heart of the redox hub. *Plant Physiol.* 155 (1), 2–18.
- Grasshoff, K., Kremling, K., Ehrhardt, M., 1999. *Methods of Seawater Analysis*. Wiley-VCH, Weinheim (FRG).
- Guillard, R.R.L., Cassie, V., 1963. Minimum cyanocobalamin requirements of some marine centric diatoms. *Limnol. Oceanogr.* 8, 161–165.
- Hauss, H., Franz, J.M.S., Hansen, T., Struck, U., Sommer, U., 2013. Relative inputs of upwelled and atmospheric nitrogen to the eastern tropical North Atlantic food web: spatial distribution of δ¹⁵N in mesozooplankton and relation to dissolved nutrient dynamics. *Deep-Sea Res. I Oceanogr. Res. Pap.* 75, 135–145.
- Hem, J.D., Roberson, C.E., Lind, C.J., 1985. Thermodynamic stability of CoOOH and its coprecipitation with manganese. *Geochim. Cosmochim. Acta* 49 (3), 801–810.
- Hewson, I., et al., 2009. In situ transcriptomic analysis of the globally important keystone N₂-fixing taxon *Crocospaera watsonii*. *ISME J.* 3 (5), 618–631.
- Hopkinson, B.M., Morel, F.M.M., 2009. The role of siderophores in iron acquisition by photosynthetic marine microorganisms. *Biometals* 22 (4), 659–669.
- Johnson, K.S., Stout, P.M., Berelson, W.M., Sakamoto-Arnold, C.M., 1988. Cobalt and copper distributions in the waters of Santa Monica Basin, California. *Nature* 332 (6164), 527–530.
- Jothivenkatachalam, K., Chandra Mohan, S., Natarajan, P., 2013. Cobalt(III) complexes of unsaturated carboxylic acids: synthesis, characterization, and photochemical studies in aqueous medium. *Res. Chem. Intermed.* 39 (7), 3371–3386.
- Juzeniene, A., Nizauskaite, Z., 2013. Photodegradation of cobalamins in aqueous solutions and in human blood. *J. Photochem. Photobiol. B Biol.* 122, 7–14.
- Karstensen, J., Stramma, L., Visbeck, M., 2008. Oxygen minimum zones in the eastern tropical Atlantic and Pacific oceans. *Prog. Oceanogr.* 77 (4), 331–350.
- Lane, T.W., Morel, F.M.M., 2005. Regulation of carbonic anhydrase expression by zinc, cobalt, and carbon dioxide in the marine diatom *Thalassiosira weissflogii*. *Plant Physiol.* 123, 345–352.
- Lee, Y., Tebo, B.M., 1994. Cobalt(II) oxidation by the marine manganese(II)-oxidizing *Bacillus* sp. strain SG-1. *Am. Soc. Microbiol.* 60 (8), 2949–2957.
- Lin, L.-M., Huang, J.-C., Huang, D.-L., Yeh, A., 2005. The reductions of bis(terpyridyl) and ethylenediaminetetraacetato complexes of cobalt(III) by ascorbic acid. *J. Chin. Chem. Soc.* 52 (3), 455–462.
- Martell, A.E., Smith, R.M., 1976. *Critical Stability Constants: Inorganic Complexes 4*. Plenum Press, New York.
- Moffett, J.W., Ho, J., 1996. Oxidation of cobalt and manganese in seawater via a common microbially catalyzed pathway. *Geochim. Cosmochim. Acta* 60 (18), 3415–3424.
- Nazhat, N.B., Golding, B.T., Johnson, G.R.A., Jones, P., 1989. Destruction of vitamin B₁₂ by reaction with ascorbate: the role of hydrogen peroxide and the oxidation state of cobalt. *J. Inorg. Biochem.* 36 (2), 75–81.
- Noble, A.E., Saito, M.A., Maiti, K., Benitez-Nelson, C.R., 2008. Cobalt, manganese, and iron near the Hawaiian Islands: a potential concentrating mechanism for cobalt within a cyclonic eddy and implications for the hybrid-type trace metals. *Deep-Sea Res. II* 55 (10–13), 1473–1490.
- Noble, A.E., et al., 2012. Basin-scale inputs of cobalt, iron, and manganese from the Benguela-Angola front to the South Atlantic Ocean. *Limnol. Oceanogr.* 57 (4), 989–1010.
- Ogino, H., Ogino, K., 1983. Redox potentials and related parameters of Cobalt(III/II) complexes containing aminopolycarboxylates. *Inorg. Chem.* 22 (15), 2208–2211.
- Panzeca, C., et al., 2008. Potential cobalt limitation of vitamin B-12 synthesis in the North Atlantic Ocean. *Glob. Biogeochem. Cycles* 22 (2).
- Panzeca, C., et al., 2009. Distributions of dissolved vitamin B₁₂ and Co in coastal and open-ocean environments. *Estuar. Coast. Shelf Sci.* 85 (2), 223–230.
- Saito, M.A., Goepfert, T.J., 2008. Zinc–cobalt colimitation of *Phaeocystis antarctica*. *Limnol. Oceanogr.* 53 (1), 266–275.

- Saito, M.A., Moffett, J.W., 2001. Complexation of cobalt by natural organic ligands in the Sargasso Sea as determined by a new high-sensitivity electrochemical cobalt speciation method suitable for open ocean work. *Mar. Chem.* 75, 49–68.
- Saito, M.A., Moffett, J.W., 2002. Temporal and spatial variability of cobalt in the Atlantic Ocean. *Geochim. Cosmochim. Acta* 66 (11), 1943–1953.
- Saito, M.A., Moffett, J.W., Chisholm, S.W., Waterbury, J.B., 2002. Cobalt limitation and uptake in *Prochlorococcus*. *Limnol. Oceanogr.* 47 (6), 1629–1636.
- Saito, M.A., Rocap, G., Moffett, J.W., 2005. Production of cobalt binding ligands in a *Synechococcus* feature at the Costa Rica upwelling dome. *Limnol. Oceanogr.* 50 (1), 279–290.
- Saito, M.A., et al., 2010. A seasonal study of dissolved cobalt in the Ross Sea, Antarctica: micronutrient behavior, absence of scavenging, and relationships with Zn, Cd, and P. *Biogeosci. Discuss.* 7 (4), 6387–6439.
- Schlitzer, R., 2014. *Ocean Data View*.
- Sekaly, A.L.R., et al., 2002. Kinetic speciation of Co(II), Ni(II), Cu(II), and Zn(II) in model solutions and freshwaters: lability and the d electron configuration. *Environ. Sci. Technol.* 37 (1), 68–74.
- Soni, P.L., Soni, V., 2013. *Coordination Chemistry*. CRC Press; Ane Books, Boca Raton FL; New Delhi.
- Suárez-Suárez, A., Tovar-Sánchez, A., Rosselló-Mora, R., 2011. Determination of cobalamins (hydroxo-, cyano-, adenosyl- and methyl-cobalamins) in seawater using reversed-phase liquid chromatography with diode-array detection. *Anal. Chim. Acta.* 701 (1), 81–85.
- Zhang, H., Van den Berg, C.M.G., Wollast, R., 1990. The determination of interactions of cobalt(II) with organic compounds in seawater using cathodic stripping voltammetry. *Mar. Chem.* 28, 285–300.